



**HAL**  
open science

## **Clostridium difficile Has an Original Peptidoglycan Structure with a High Level of N-Acetylglucosamine Deacetylation and Mainly 3-3 Cross-links**

Johann J. Peltier, Pascal P. Courtin, Imane I. El Meouche, Ludovic L. Lemeé, Marie-Pierre Chapot-Chartier, Jean-Louis J.-L. Pons

► **To cite this version:**

Johann J. Peltier, Pascal P. Courtin, Imane I. El Meouche, Ludovic L. Lemeé, Marie-Pierre Chapot-Chartier, et al.. Clostridium difficile Has an Original Peptidoglycan Structure with a High Level of N-Acetylglucosamine Deacetylation and Mainly 3-3 Cross-links. *Journal of Biological Chemistry*, 2011, 286 (33), pp.29053 - 29062. 10.1074/jbc.M111.259150 . hal-01004568

**HAL Id: hal-01004568**

**<https://hal.science/hal-01004568>**

Submitted on 29 May 2020

**HAL** is a multi-disciplinary open access archive for the deposit and dissemination of scientific research documents, whether they are published or not. The documents may come from teaching and research institutions in France or abroad, or from public or private research centers.

L'archive ouverte pluridisciplinaire **HAL**, est destinée au dépôt et à la diffusion de documents scientifiques de niveau recherche, publiés ou non, émanant des établissements d'enseignement et de recherche français ou étrangers, des laboratoires publics ou privés.

Copyright

# *Clostridium difficile* Has an Original Peptidoglycan Structure with a High Level of *N*-Acetylglucosamine Deacetylation and Mainly 3-3 Cross-links<sup>\*[S]</sup>

Received for publication, May 9, 2011, and in revised form, June 7, 2011. Published, JBC Papers in Press, June 17, 2011, DOI 10.1074/jbc.M111.259150

Johann Peltier<sup>‡</sup>, Pascal Courtin<sup>§¶</sup>, Imane El Meouche<sup>‡</sup>, Ludovic Lemée<sup>‡</sup>, Marie-Pierre Chapot-Chartier<sup>§¶</sup>, and Jean-Louis Pons<sup>‡1</sup>

From the <sup>‡</sup>Laboratoire G.R.A.M., EA 2656 IFR 23, Rouen University Hospital, 22 Boulevard Gambetta, 76183 Rouen Cedex, France, <sup>§</sup>the Institut National de la Recherche Agronomique, UMR1319 Micalis, F-78350 Jouy-en-Josas, France, and <sup>¶</sup>AgroParisTech, UMR Michalis, F-78350 Jouy-en-Josas, France

The structure of the vegetative cell wall peptidoglycan of *Clostridium difficile* was determined by analysis of its constituent muropeptides with a combination of reverse-phase high pressure liquid chromatography separation of muropeptides, amino acid analysis, mass spectrometry and tandem mass spectrometry. The structures assigned to 36 muropeptides evidenced several original features in *C. difficile* vegetative cell peptidoglycan. First, it is characterized by a strikingly high level of *N*-acetylglucosamine deacetylation. In addition, the majority of dimers (around 75%) contains A<sub>2</sub>pm<sup>3</sup> → A<sub>2</sub>pm<sup>3</sup> (A<sub>2</sub>pm, 2,6-diaminopimelic acid) cross-links and only a minority of the more classical Ala<sup>4</sup> → A<sub>2</sub>pm<sup>3</sup> cross-links. Moreover, a significant amount of muropeptides contains a modified tetrapeptide stem ending in Gly instead of D-Ala<sup>4</sup>. Two L<sub>D</sub>-transpeptidases homologues encoding genes present in the genome of *C. difficile* 630 and named *ldt<sub>cd1</sub>* and *ldt<sub>cd2</sub>*, were inactivated. The inactivation of either *ldt<sub>cd1</sub>* or *ldt<sub>cd2</sub>* significantly decreased the abundance of 3-3 cross-links, leading to a marked decrease of peptidoglycan reticulation and demonstrating that both *ldt<sub>cd1</sub>*- and *ldt<sub>cd2</sub>*-encoded proteins have a redundant L<sub>D</sub>-transpeptidase activity. The contribution of 3-3 cross-links to peptidoglycan synthesis increased in the presence of ampicillin, indicating that this drug does not inhibit the L<sub>D</sub>-transpeptidation pathway in *C. difficile*.

*Clostridium difficile*, a Gram-positive spore-forming bacterium, is the major cause of intestinal diseases associated with antibiotic therapy such as ampicillin, clindamycin, and cephalosporins, which disrupt the barrier intestinal flora and allow *C. difficile* colonization (1, 2). Clinical manifestations range from asymptomatic colonization or mild diarrhea to pseudomembranous colitis (3). The main virulence factors have been identified as toxin A and B (4). Recent outbreaks have led to increasing morbidity and mortality and have been associated with a new highly virulent strain (BI/NAP1/027) of *C. difficile*.

\* This work was supported by the University of Rouen and Rouen University Hospital.

[S] The on-line version of this article (available at <http://www.jbc.org>) contains supplemental Tables S1 and S2 and Figs. S1–S3.

<sup>1</sup> To whom correspondence should be addressed: Groupe de Recherche sur les Antimicrobiens et les Micro-organismes, UPRES EA2656, IFR23, Université de Rouen, 22 Boulevard Gambetta, F-76183 Rouen Cedex, France. Tel.: 33-235-148-452; Fax: 33235-148-203; E-mail: jean-louis.pons@univ-rouen.fr.

Antibiotic treatment of *C. difficile*-associated disease requires metronidazole or vancomycin therapy.

Peptidoglycan (PG)<sup>2</sup> of Gram-positive bacteria usually consists of long linear glycan strands cross-linked by short stem peptides (5, 6). PG is usually connected by 4-3 cross-links catalyzed by D<sub>D</sub>-transpeptidases, which belong to the penicillin-binding proteins and whose substrate is the peptidyl D-Ala<sup>4</sup>-D-Ala<sup>5</sup> extremity of PG precursors. D<sub>D</sub>-Transpeptidases are the essential targets of β-lactams antibiotics, which are structural analogues of the D-Ala<sup>4</sup>-D-Ala<sup>5</sup> terminus precursor molecule (7, 8). Alternatively, PG can be connected by 3-3 cross-links generated by L<sub>D</sub>-transpeptidases (9), which were originally detected in *Enterococcus faecium* (Ldt<sub>fm</sub>) (10) and then in other Gram-positive bacteria (11, 12), in mycobacteria (13–15), and in *Escherichia coli* (16, 17). Ldts use acyl donors containing a tetrapeptide stem (9) and were consequently expected to confer resistance to β-lactams (10, 18).

Another possible variation of the PG structure is the occurrence of *N*-deacetylation or *O*-acetylation of glycan strands, either on GlcNAc or on MurNAc residues (19, 20). *N*-Deacetylation in *Listeria monocytogenes* (21) or *Streptococcus pneumoniae* (22) and *O*-acetylation in *Staphylococcus aureus* have been linked to lysozyme resistance (23).

The PGs of *C. difficile* should have some specificities regarding the effect of antibiotics inhibiting PG biosynthesis; *C. difficile*, although susceptible to β-lactams, exhibits higher minimal inhibitory concentrations than in other *Clostridium* species such as *Clostridium perfringens* (24), and it also displays a preserved susceptibility to vancomycin despite the presence of a *vanG*-like operon (25). However, little is known about the PG structure and biosynthesis in *C. difficile*. In the present work, we report the fine structure of *C. difficile* vegetative PG. This structure reveals the presence of a high proportion of non-acetylated glucosamine residues on the glycan strands and the unusual abundance of 3 → 3 peptide cross-links generated by L<sub>D</sub>-transpeptidation. Mutations of two putative L<sub>D</sub>-transpeptidase genes demonstrate the role of the corresponding proteins in the formation of 3 → 3 cross-links. The participation of the L<sub>D</sub>-transpeptidases to peptidoglycan cross-linking increases in

<sup>2</sup> The abbreviations used are: PG, peptidoglycan; RAM, retrotransposition-activated marker; A<sub>2</sub>pm, 2,6-diaminopimelic acid; GlcNH<sub>2</sub>, *N*-deacetylated GlcNAc; MurOHNAc, *N*-acetylmuramicitol; MurNac, *N*-acetylmuramic acid; GlcNac, *N*-acetylglucosamine.

## Peptidoglycan Structure of *Clostridium difficile*

the presence of ampicillin, indicating that this drug does not inhibit the L,D-transpeptidation pathway in *C. difficile*.

### EXPERIMENTAL PROCEDURES

**Bacterial Strains and Culture Conditions**—The bacterial strains used in this study are listed in [supplemental Table S1](#). *C. difficile* 630, which is a virulent and multidrug-resistant isolated from an outbreak in Switzerland (25), and *C. difficile* 630 $\Delta$ erm (26), which is a spontaneously cured derivative of strain 630 and allows selection of ClosTron mutants, were used in all experiments. *C. difficile* strains were routinely cultured on blood agar (Oxoid), BHI agar (Difco), or BHI broth (Difco) at 37 °C in an anaerobic environment (80% N<sub>2</sub>, 10% CO<sub>2</sub>, and 10% H<sub>2</sub>). When necessary, *C. difficile* culture media were supplemented with cefoxitin (25 mg/liter), thiamphenicol (15 mg/liter), or erythromycin (5 mg/liter). *E. coli* Top10 (Invitrogen) was used for cloning and plasmid propagation, and *E. coli* HB101 (RP4) was used as the conjugative donor strain employed in the creation of *C. difficile* mutants. *E. coli* strains were cultured aerobically at 37 °C in LB broth or LB agar (MP Biomedicals) containing chloramphenicol (25 mg/liter). When required, ampicillin (100 mg/liter) was added.

**Susceptibility Testing**—Minimal inhibitory concentrations for ampicillin and vancomycin against *C. difficile* strains were determined by the E-test method (Bio-Merieux) from bacterial suspensions at 3 Mc-Farland turbidity.

**Peptidoglycan Structure Analysis**—*C. difficile* PG structure was analyzed by reverse-phase high performance liquid chromatography (RP-HPLC) and matrix-assisted laser desorption ionization-time of flight (MALDI-TOF) mass spectrometry as described previously for *Lactococcus lactis* (27) with some modifications. Briefly, PG was extracted from an exponential culture (A<sub>600</sub> of 0.3) on BHI with boiling sodium dodecyl sulfate and was deproteinized by treatment with Pronase and trypsin. The material was treated with DNase (50  $\mu$ g/ml) and RNase (50  $\mu$ g/ml) and then incubated with 48% hydrofluoric acid at 4 °C for 16 h to remove cell-wall teichoic acids. Purified PG was digested with mutanolysin (Sigma), and the soluble muropeptides were reduced with sodium borohydride. They were then separated by RP-HPLC using a Hypersil octyldecyl silane column (C<sub>18</sub>; 250  $\times$  4.6 mm; 5  $\mu$ m; ThermoHypersil-Keystone) at 50 °C by the method of Courtin *et al.* (27). Fractions containing the main peaks were analyzed by MALDI-TOF mass spectrometry with a Voyager DE STR mass spectrometer (Applied Biosystems) and  $\alpha$ -cyano-4-hydroxycinnamic acid matrix.

**Amino Acid and Amino Sugar Composition Analysis**—Amino acid and amino sugar composition analysis of muropeptides after acid hydrolysis was performed using the previously described Waters Picotag method (27).

**Tandem Mass Spectrometry**—For MS-MS structural analysis, muropeptides were desalted on a Betasil C18 column (4.6  $\times$  250 mm, Thermo Electron Corp.) with acetonitrile/formic acid buffer system and dried with speed-vacuum. Samples were solubilized in 2% acetonitrile, 0.1% formic acid in milliQ water (1  $\mu$ l for 1 milliabsorbance unit detected at 214 nm in the previous HPLC system). Each purified muropeptide was injected and analyzed at a flow rate of 0.2  $\mu$ l/min in the mass spectrometers (LTQ-ETD or LTQ-Orbitrap, Thermo Fisher) located on the

PAPPSO platform (Institut National de la Recherche Agronomique, France).

**General DNA Techniques**—Chromosomal DNA extraction from *C. difficile* colonies was performed using the InstaGene Matrix kit (Bio-Rad). PCRs were done with a reaction volume of 25  $\mu$ l by using GoTaq Green Master (Promega) or Advantage II Polymerase Mix (BD Biosciences). The primers used (Eurofins MWG Operon) are listed in [supplemental Table S2](#). PCR products and plasmids were purified using a NucleoSpin Extract II kit and a Nucleospin plasmid kit (Macherey-Nagel), respectively.

**Construction of *C. difficile* *ldt*<sub>cd1</sub> and *ldt*<sub>cd2</sub> Single Mutants by Using the ClosTron System**—The ClosTron system was used as described previously (28) in conjunction with the commercially available TargeTron gene knock-out system kit (Sigma). Briefly, the algorithm available on the TargeTron Design Site was used to identify intron insertion sites within *ldt*<sub>cd1</sub> and *ldt*<sub>cd2</sub>. The primers ([supplemental Table S2](#)) designed by the algorithm to retarget the group II intron on pMTL007 to *ldt*<sub>cd1</sub> and *ldt*<sub>cd2</sub> were used with the EBS universal primer and intron template DNA to generate a 353-bp DNA fragment for each gene by overlap PCR according to the manufacturer's instructions. The two resultant PCR products were cloned into the HindIII and BsrGI restriction sites of pMTL007, and the constructs were transformed into *E. coli* TOP10. The fidelity of the cloned inserts was verified by DNA sequencing using pMTL007-specific primers pMTLseq-F and pMTLseq-R ([supplemental Table S2](#)). pMTL007::Cdi-*ldt*<sub>cd1</sub>-1231s and pMTL007::Cdi-*ldt*<sub>cd2</sub>-480s plasmids ([supplemental Table S2](#)) retargeted the group II intron to insert into *ldt*<sub>cd1</sub> and *ldt*<sub>cd2</sub> genes in the sense orientation immediately after the 1231th and 480th nucleotides in the coding sequence, respectively, thus within the DNA sequence encoding the catalytic domain. These derivative pMTL007 plasmids were transformed into the conjugative donor *E. coli* HB101 (RP4) and then transferred via conjugation into the *C. difficile* 630 $\Delta$ erm. Successful *C. difficile* transconjugants were selected by subculturing on BHI agar containing cefoxitin (25 mg/liter) and thiamphenicol (15 mg/liter). Then, the integration of the group II intron RNA into the *ldt*<sub>cd1</sub> and *ldt*<sub>cd2</sub> genes was selected by plating onto BHI agar with erythromycin (5 mg/liter). Erythromycin-resistant (and thiamphenicol-sensitive) *C. difficile* colonies are produced after plasmid loss and insertion of the group II intron into the chromosome, which is accompanied by splicing out of the group I intron from the *ermB* retrotransposition-activated marker (RAM). Moreover, genomic DNA of erythromycin-resistant transconjugants was isolated and subjected to PCR using primers flanking *ldt*<sub>cd1</sub>*ldt*<sub>cd1</sub>-F and *ldt*<sub>cd1</sub>-R ([supplemental Table S2](#)) and primers flanking *ldt*<sub>cd2</sub>*ldt*<sub>cd2</sub>-F and *ldt*<sub>cd2</sub>-R ([supplemental Table S2](#)) to verify that the group II intron had inserted into the correct target gene. In addition to Erm resistance being demonstrated phenotypically, confirmatory PCR using the RAM-F/RAM-R primer pair ([supplemental Table S2](#)) was also performed.

**Construction of a *C. difficile* *ldt*<sub>cd1</sub> and *ldt*<sub>cd2</sub> Double Mutant by Using the ClosTron System**—The *ldt*<sub>cd1</sub>-*ldt*<sub>cd2</sub> double mutant was constructed from the *ldt*<sub>cd2</sub> single mutant. Retargeted plasmid pMTL007::Cdi-*ldt*<sub>cd1</sub>-1231s was transferred via conjugation,

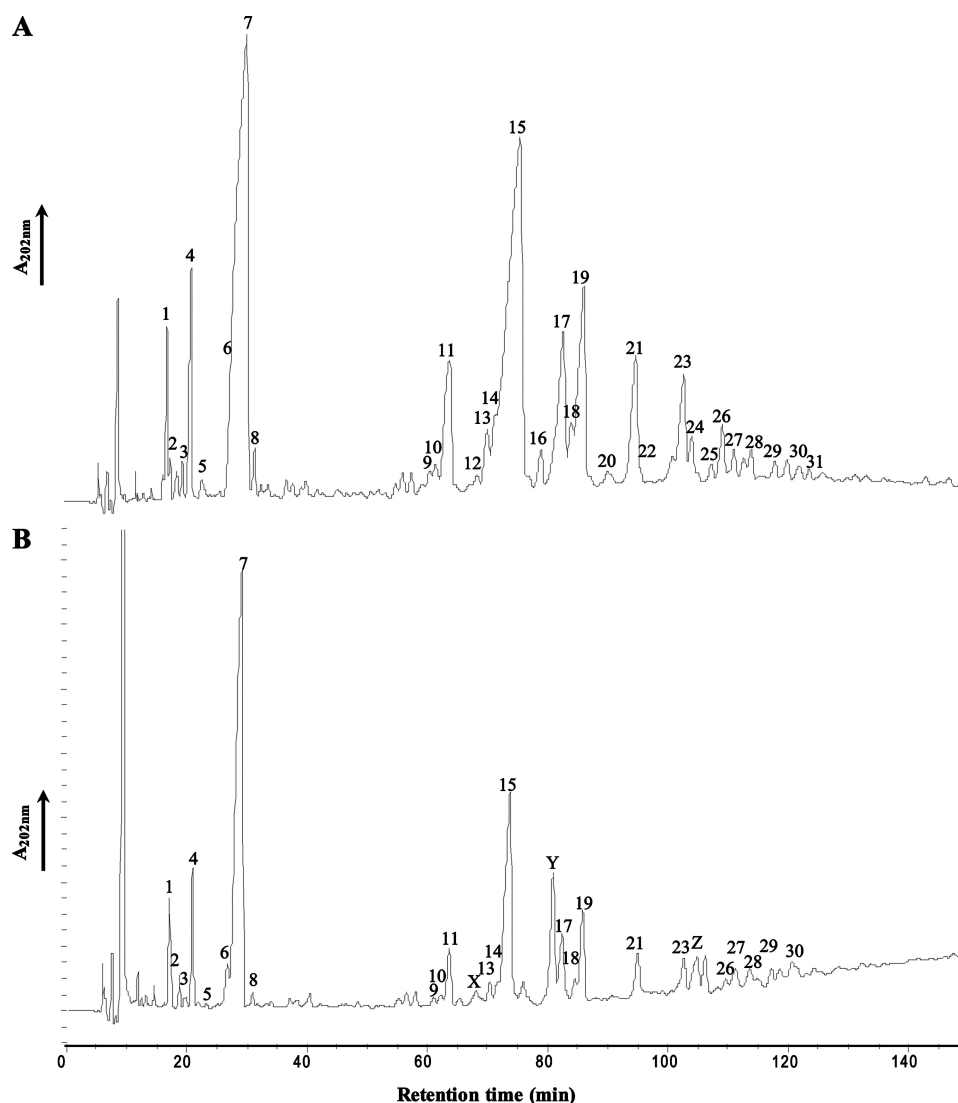


FIGURE 1. RP-HPLC separation of mucopeptides from *C. difficile* 630 (A) and from *C. difficile* 630 $\Delta$ erm *ldt<sub>cd1</sub>::intron-erm* (B). Peaks numbers refer to Table 1. A few peaks contain two mucopeptides identified as *a* and *b* in Table 1. New mucopeptides identified in the *ldt<sub>cd1</sub>* mutant strain are referred as X, Y, and Z.

as previously, into the *C. difficile* 630 $\Delta$ erm *ldt<sub>cd1</sub>::intron-erm*. *C. difficile* transconjugants were selected by subculturing on BHI agar containing thiamphenicol (15  $\mu$ g/ml). The double mutant could not be selected by erythromycin resistance, as a functional *ermB* gene was carried in the single mutant strain. Consequently, intron insertion was directly screened by PCR. Genomic DNA was isolated from single thiamphenicol-resistant colonies and subjected to PCR using primer *ldt<sub>cd1</sub>*-F with the EBS universal primer (supplemental Table S2) to determine the presence of an intron insertion. As low frequency of intron insertion was detected within the first tested transconjugants, several re-streaking of colonies onto fresh BHI agar containing thiamphenicol (15 mg/liter) were necessary. Positive individual colonies were tested by PCR using *ldt<sub>cd1</sub>*-flanking primers (supplemental Table S2).

## RESULTS

**Vegetative Cell Wall Peptidoglycan Composition of *C. difficile* 630**—Mucopeptides of *C. difficile* 630 were obtained from PG digestion by muramidase mutanolysin, reduced with sodium

borohydride, and separated by RP-HPLC. The HPLC mucopeptide profile is presented on Fig. 1A. PG extracted from exponential and stationary phases cultures ( $A_{600\text{ nm}}$  of 0.35 and 1.4, respectively) displayed similar elution profiles of mucopeptides. Amino acid and amino sugar composition analysis of the major peaks 4, 7, 11a, and 15a after acid hydrolysis, using the Waters Picotag method (27), confirmed mucopeptides with Ala, Glu, A<sub>2</sub>pm (2,6-diaminopimelic acid), and in some cases Gly (data not shown). The mass of 31 peaks was determined by MALDI-TOF mass spectrometry, and the structure of 36 mucopeptides was deduced (Table 1). The structure of mucopeptides and their respective abundances, expressed as percentages of the area under all of the mucopeptides peaks, are presented in Table 1. Monomers, dimers, and trimers represented 35.1, 56.6, and 8.3% of the total Mucopeptides, respectively, and the cross-linking index was calculated to be 33.8% (Table 2). AnhydroMurNAc mucopeptides, proposed to be present at the extremity of glycan chains (29), were detected in low amounts (peaks 30 and 31) (Table 1).



# Peptidoglycan Structure of *Clostridium difficile*

**TABLE 1**

Structures, molecular masses, and proportions of muropeptides from *C. difficile* 630 grown in BHI, in BHI plus ampicillin, and from *ldt<sub>cd1</sub>*, *ldt<sub>cd2</sub>*, and *ldt<sub>cd1</sub>ldt<sub>cd2</sub>* mutant strains

NA, Not applicable; ND, Not determined.

Peak <sup>a</sup>	Proposed structures <sup>b</sup>	<i>m/z</i> [M+Na] <sup>+c</sup>		Cross-link	% of all peaks <sup>d</sup>				
		Observed	Calculated		630	630+Ampi	Mutant		
							<i>ldt<sub>cd1</sub></i>	<i>ldt<sub>cd2</sub></i>	<i>ldt<sub>cd1</sub>ldt<sub>cd2</sub></i>
<b>Monomers</b>									
1	Tri (deAc)	851.30	851.35	NA	35.1	33.6	49.8	46.9	51.5
2	Tetra missing GlcNAc	761.28	761.33	NA	1.9	2.6	3.4	2.5	2.6
3	Tri-Gly (deAc)	950.30	950.41	NA	0.4	0.7	0.2	0.4	1.1
4	Tri-Gly (deAc)	908.38	908.40	NA	0.4	0.4	0.1	0.4	0.4
6	Tetra	964.44	964.40	NA	3.1	4.8	2.1	3.7	2.0
7	Tetra (deAc)	922.44	922.39	NA	2.4	1.7	3.6	1.9	1.4
8	Di (deAc)	679.30	679.26	NA	26.3	22.5	39.9	37.6	43.5
<b>Dimers</b>									
5a	Tri-Tri-Gly (deAc) missing Ds	1280.38	1280.56	3-3	56.6	56.0	41.3	44.3	41.5
5b	Tri-Tri (deAc) missing Ds	1223.37	1223.50	3-3	0.4 <sup>e</sup>	0.2 <sup>e</sup>	0.1 <sup>e</sup>	0.1 <sup>e</sup>	0.1 <sup>e</sup>
9	Tri-Tri-Gly (deAc)	1760.56	1760.75	3-3	0.3	0.7	0.4	0.3	0.3
10	Tri-Tetra (deAc) missing GlcNAc	1571.58	1571.66	3-3	0.5	1.2	0.6	0.6	0.6
11a	Tri-Tri-Gly (deAc ×2)	1718.54	1718.74	3-3	4.7 <sup>e</sup>	6.9 <sup>e</sup>	1.6 <sup>e</sup>	3.0 <sup>e</sup>	1.8 <sup>e</sup>
11b	Tri-Tri (deAc ×2)	1661.81	1661.68	3-3	0	0	0	0	0
12	Tri-Tetra	1816.80	1816.76	ND	0.2	0.4	0	0	0
X	Tri-Tetra (deAc ×2)	1730.51	1730.51	No <sup>f</sup>	0	0	0.9	0.6	0.7
13	Tri-Tetra (deAc)	1774.74	1774.75	3-3	1.5	1.8	0.8	0.9	0.9
14	Tri-Tetra (deAc)	1774.70	1774.75	3-3	1.9	3.1	0.7	0.9	0.9
15a	Tri-Tetra (deAc ×2)	1732.77	1732.74	3-3	24.8	24.1 <sup>e</sup>	11.7	16.0	13.8
15b	Tri-Gly-Tetra (deAc ×2)	1789.76	1789.79	4-3	1.4	1.4	1.4	1.4	1.4
16	Tri-Tetra (deAc)	1774.56	1774.75	3-3	0.8	3.5	0	0	0.4
Y	Tetra-Tetra (deAc ×2)	1801.70	1801.70	No <sup>f</sup>	0	0	10.5	7.1	6.5
17	Tri-Tetra (deAc ×2)	1732.67	1732.74	3-3	6.2	6.7	3.1	3.9	3.9
18	Tetra-Tetra (deAc)	1845.72	1845.78	4-3	1.6	0.6	1.3	1.0	1.4
19	Tetra-Tetra (deAc ×2)	1803.73	1803.77	4-3	7.2	2.4	5.2	5	5.5
20	Tetra-Tetra (deAc)	1845.66	1845.78	4-3	0.4	0.2	0	0	0
21	Tetra-Tetra (deAc ×2)	1803.66	1803.77	4-3	4.1	2.4	2.1	2.3	2.5
30	Tri-Tetra-Anh (deAc)	1754.72	1754.72	ND	0.4	1.2	0.9	1.2	0.8
31	Tetra-Tetra-Anh (deAc ×2)	1783.70	1783.74	4-3	0.2	0.6	0	0	0
<b>Trimers</b>									
22a	Tri-Tri-Tri (deAc ×3)	2472.12	2472.01	ND	8.2	10.4	8.9	8.8	7.0
22b	Tri-Tri-Tri-Gly (deAc ×3)	2529.13	2529.06	ND	0.2 <sup>e</sup>	0.3	0	0	0
23	Tri-Tri-Tetra (deAc ×3)	2542.91	2543.05	ND	3.5	3.3	2	2.0	1.6
24	Tri-Tri-Tetra (deAc ×3)	2542.90	2543.05	ND	1.1	3	0	0	0
Z	Tri-Tetra-Tetra (deAc ×3)	2611.85	2611.85	ND	0	0	1.8	2.7	1.6
25	Tri-Tetra-Tetra (deAc ×2)	2656.22	2656.12	ND	0.3	0.2	0	0	0
26	Tri-Tetra-Tetra (deAc ×3)	2614.10	2614.11	ND	1.4	0.8	0.5	0.5	0.3
27	Tri-Tetra-Tetra (deAc ×3)	2613.94	2614.11	ND	0.7	1.1	1.4	1.4	1.3
28	Tri-Tetra-Tetra (deAc ×3)	2614.04	2614.11	ND	0.7	0.8	1.5	1.3	1.4
29a	Tetra-Tetra-Tetra (deAc ×3)	2685.09	2685.14	ND	0.4 <sup>e</sup>	0.9 <sup>e</sup>	1.7 <sup>e</sup>	0.9 <sup>e</sup>	0.8 <sup>e</sup>
29b	Tetra-Tetra-Tetra (deAc ×2)	2727.12	2727.15	ND					

<sup>a</sup> Peak numbers refer to Fig. 1. A few peaks contain two muropeptides, named a and b.

<sup>b</sup> Di, disaccharide dipeptide (L-Ala-D-Glu); Tri, disaccharide tripeptide (L-Ala-D-Glu-A<sub>2</sub>pm); Tetra, disaccharide tetrapeptide (L-Ala-D-Glu-A<sub>2</sub>pm-D-Ala); Ds, disaccharide, GlcNAc-MurNAc; deAc, deacetylation; Anh, Anhydro.

<sup>c</sup> Sodiated molecular ions were the most abundant on MALDI-TOF mass spectra for all muropeptides. *m/z* values correspond to monoisotopic masses.

<sup>d</sup> Percentage of each peak was calculated as the ratio of the peak area over the sum of areas of all the peaks identified in the table.

<sup>e</sup> Relative percentage of peaks a and b was not determined.

<sup>f</sup> No, absence of cross-link.

***N*-Deacetylation of Peptidoglycan Glycan Strands**—Among the muropeptides identified, a high proportion had one or more 42-Da mass defects compared with the expected calculated molecular masses. This 42-Da mass defect suggests a lack of one acetyl group on an amino sugar. To determine if this *N*-deacetylation occurs on GlcNAc or MurNAc, the major dimer peak 15a (*m/z* 855.9, *z* = 2), containing a muropeptide dimer with two *N*-deacetylations, was subjected to MS-MS analysis (Fig. 2). Among the muropeptide fragment ions, fragments with an *m/z* of 775.3 (*z* = 2) and *m/z* of 694.9 (*z* = 2) corresponded to the loss of 1 (mass defect of 161 Da) or 2 glucosamines, respectively. In contrast, no fragment corresponding to the loss of one GlcNAc (mass defect of 203 Da) was observed. In addition, fragments resulting from the loss of one MurNAc (mass defect of 277 Da) were observed, whereas no fragment corresponding to the loss of one muramic acid (mass defect of 235 Da) was

visualized. These results indicate that muropeptide 15a contains two glucosamine residues instead of GlcNAc residues. MS-MS analyses of the main monomers (muropeptides 4 and 7) and subsequent MS-MS analyses of the main dimers realized in this study (muropeptides 10, 11a, 11b, 13, 14, 15a, 15b, 16, 17, 19, 21) were in agreement with this result, indicating that the 42-Da defect always corresponds to *N*-deacetylation of glucosamine. Overall, 93% of the GlcNAc residues were *N*-deacetylated in the PG of *C. difficile*.

**Relative Proportions of 3-3 and 4-3 Cross-links in the Peptidoglycan**—On the basis of MALDI-TOF mass determination, muropeptide 11b was proposed to have a dimer structure with two tripeptide stems, strongly suggesting a cross-link between two A<sub>2</sub>pm residues (3-3 cross-link), generated by L,D-transpeptidation. This structure was confirmed by MS-MS analysis, as a fragment ion with *m/z* of

TABLE 2

Relative distribution (%) of muuropeptides in *C. difficile* 630 grown in BHI, in BHI plus ampicillin, and from *ldt<sub>cd1</sub>*, *ldt<sub>cd2</sub>*, and *ldt<sub>cd1</sub>ldt<sub>cd2</sub>* mutant strains. Percentages were calculated from the values shown in Table I.

Muropeptide	Strains				
	630	630 + Ampicillin	<i>ldt<sub>cd1</sub></i> mutant	<i>ldt<sub>cd2</sub></i> mutant	<i>ldt<sub>cd1</sub>ldt<sub>cd2</sub></i> mutant
Monomers	35.1	33.6	49.8	46.9	51.5
<b>Dimers</b>	56.6	56	29.9	36.6	34.3
3-3 Cross-link <sup>a</sup>	41.3	48.6	19	25.7	22.7
4-3 Cross-link	15.3	7.4	10.9	10.9	11.6
No cross-link (peaks X and Y)	0	0	11.4	7.7	7.2
<b>Trimers</b>	8.3	10.4	8.9	6	5.4
One cross-link (peak Z)	0	0	1.8	2.7	1.6
Cross-linking index <sup>b</sup>	33.8	34.9	18.2	21.5	19.8

<sup>a</sup> Percentages were calculated using muuropeptides dimers with determined 3-3 cross-link.

<sup>b</sup> The cross-linking index was calculated with the formula  $(1/2\sum \text{dimers} + 2/3\sum \text{trimers})/\sum \text{all muuropeptides}$  (44). Dimers without cross-link were accounted as two monomers. In the same way, trimers with only one cross-link were accounted as one dimer and one monomer.

363.2 and corresponding to an A<sub>2</sub>pm- A<sub>2</sub>pm dipeptide was observed (Fig. 3). Among dimers, muuropeptides 5b had also two tripeptide stems and clearly contained the unusual A<sub>2</sub>pm<sup>3</sup> → A<sub>2</sub>pm<sup>3</sup> cross-link.

As cross-links generated by L<sub>D</sub>-transpeptidation were detected in the PG of *C. difficile*, MS-MS analysis of the main dimers were performed to differentiate D-Ala<sup>4</sup> → A<sub>2</sub>pm<sup>3</sup> and A<sub>2</sub>pm<sup>3</sup> → A<sub>2</sub>pm<sup>3</sup> cross-links generated by transpeptidases of D<sub>D</sub> and L<sub>D</sub> specificities, respectively. Major dimeric muuropeptide 15a may contain either 4 → 3 (donor tetrapeptide stem and acceptor tripeptide stem) or 3 → 3 cross-links (donor tripeptide stem and acceptor tetrapeptide stem). The fragmentation pattern of the muuropeptide 15a revealed a 3 → 3 cross-link as 1 alanine residue was lost (mass defect of 89 Da) from the C-terminal end of the acceptor tetrapeptide stem. Moreover, a fragment ion with *m/z* of 474.3 corresponding to Glu-A<sub>2</sub>pm-A<sub>2</sub>pm was observed, confirming the A<sub>2</sub>pm<sup>3</sup> → A<sub>2</sub>pm<sup>3</sup> cross-link (Fig. 2). Muuropeptides 10, 13, 14, 16, and 17 have also a dimer structure with a tripeptide stem and a tetrapeptide stem. Interestingly, MS-MS analysis of these muuropeptides revealed the presence of an A<sub>2</sub>pm<sup>3</sup> → A<sub>2</sub>pm<sup>3</sup> cross-link in all cases.

Seven identified muuropeptides contain glycine in their composition (muuropeptides 3, 4, 5a, 9, 11a, 15b, and 22b). Analysis of muuropeptide 11a by MS-MS showed that Gly was linked with A<sub>2</sub>pm (supplemental Fig. S1). Moreover, the fragmentation pattern indicated that the muuropeptide 11a harbors an A<sub>2</sub>pm<sup>3</sup> → A<sub>2</sub>pm<sup>3</sup> cross-link generated by L<sub>D</sub>-transpeptidation. Thus, glycine does not constitute an interpeptide bridge with the adjacent peptide subunit but is located at position 4 of a peptide stem instead of D-Ala. This result suggests that L<sub>D</sub>-transpeptidases of *C. difficile* 630 could hydrolyze D-Ala<sup>4</sup> and exchange this residue with Gly, as shown in *E. coli* (17). In this way dimers with a disaccharide tripeptide stem and a disaccharide tetrapeptide stem ending in Gly (peaks 5a, 9, and 11a) were considered to contain an A<sub>2</sub>pm<sup>3</sup> → A<sub>2</sub>pm<sup>3</sup> cross-link. Conversely, MS-MS analysis of the dimer 15b, which harbors a tetrapeptide stem and a tetrapeptide ending in Gly, was shown to contain an Ala<sup>4</sup> → A<sub>2</sub>pm<sup>3</sup> cross-link (data not shown). Dimers 18, 19, 20, 21, and 31 were proposed to have a dimer structure with a donor tetrapeptide stem and an acceptor tetrapeptide stem, suggesting they contained 4 → 3 cross-links. As expected, the fragmentation patterns of muuropeptides 19 and 21 showed that the cross-link was of the Ala<sup>4</sup> → A<sub>2</sub>pm<sup>3</sup> type (supplemental Fig.

S2 and data not shown). Muuropeptides 18, 20, and 31 were considered to also contain 4 → 3 cross-links.

Thus, the PG of *C. difficile* contains both D-Ala<sup>4</sup> → A<sub>2</sub>pm<sup>3</sup> cross-links generated by D<sub>D</sub>-transpeptidation and A<sub>2</sub>pm<sup>3</sup> → A<sub>2</sub>pm<sup>3</sup> cross-links generated by L<sub>D</sub>-transpeptidation. For the whole muuropeptides, the proportion of dimers generated by L<sub>D</sub>-transpeptidation and D<sub>D</sub>-transpeptidation were about 41.3 and 15.3% that of the area of all peaks, respectively (Table 2). Therefore, 73% of the cross-links of the dimeric muuropeptides were generated by L<sub>D</sub>-transpeptidation.

*Inactivation of Two Putative L<sub>D</sub>-Transpeptidases Encoding Genes Using the ClosTron System*—The genome of *C. difficile* contains a gene named *ldt<sub>cd1</sub>* (CD2963) that encodes a protein of 469 residues, related to Ldt<sub>fm</sub> of *E. faecium* (overall amino acid identity, 29%; amino acid identity for the catalytic domain, 38%). The two proteins display the same domain composition, including a putative transmembrane domain, two putative PG binding domains belonging to PG binding 4 superfamily, and the catalytic domain with the SXGC conserved motif (Fig. 4) (10, 30). Two others proteins, Ldt<sub>cd2</sub> (CD2713) and CD3007, encoded by the *C. difficile* genome, exhibit significant sequence identity with the Ldt<sub>fm</sub> catalytic domain (25 and 23%, respectively), including the SXGC motif (Fig. 4). Unlike Ldt<sub>fm</sub> and Ldt<sub>cd1</sub>, Ldt<sub>cd2</sub> and CD3007 have no hydrophobic regions that could act as membrane anchors but contain a putative peptidoglycan binding domain consisting of three CWB-2 modules or two SH3 modules respectively.

To study the functions of the *ldt<sub>cd1</sub>* and *ldt<sub>cd2</sub>* genes, the ClosTron system was used to create insertional mutants of *C. difficile* 630Δ*erm* in which either the *ldt<sub>cd1</sub>* or *ldt<sub>cd2</sub>* gene or both *ldt<sub>cd1</sub>ldt<sub>cd2</sub>* genes were inactivated. Insertion of the group II intron into the target genes was verified by PCR using specific internal primers (supplemental Table S2 and Fig. S3). For unknown reasons and despite multiple attempts, it was not possible to inactivate the CD3007 encoding gene using the ClosTron system.

*Effect of ldt<sub>cd1</sub> Mutation, ldt<sub>cd2</sub> Mutation, or ldt<sub>cd1</sub>-ldt<sub>cd2</sub> Double Mutation on the Peptidoglycan Structure*—The growth rate of the different mutant strains was not impaired when compared with that of the parental strain. To determine the role of the putative L<sub>D</sub>-transpeptidase Ldt<sub>cd1</sub>, the PG structure of the corresponding mutant strain was determined and compared with the muuropeptide profile of the *C. difficile* 630Δ*erm* parental strain (of

## Peptidoglycan Structure of *Clostridium difficile*

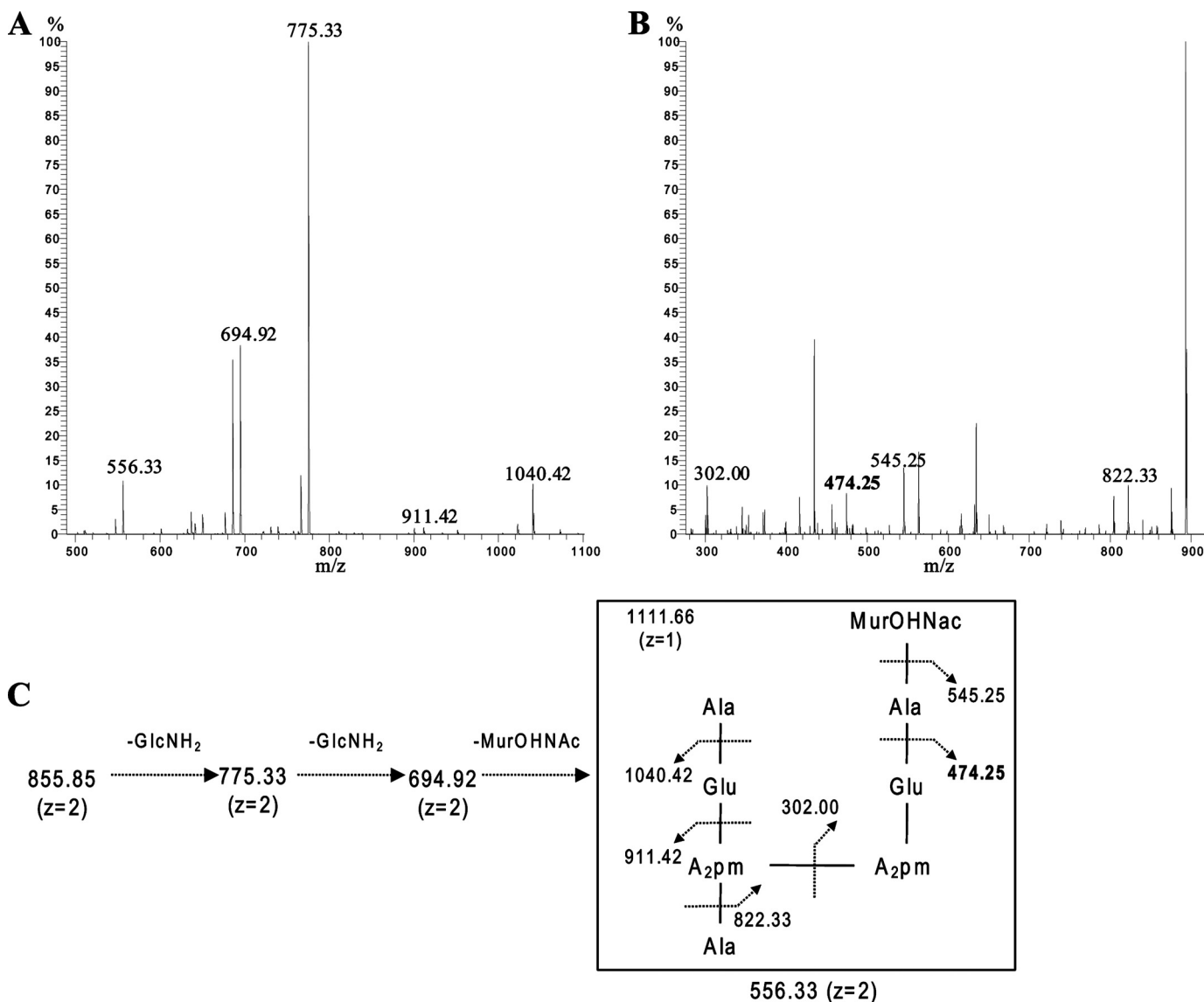


FIGURE 2. **Sequencing of muropeptide 15a by MS-MS.** The muropeptide was desalted and analyzed by MS-MS with a MALDI source. The parental ion ( $m/z$  855.85 with  $z = 2$ ) (A) and the fragment ion with  $m/z$  of 911.4 (B) were selected for fragmentation. Inferred structure is represented (C). The indicated  $m/z$  values on the presented structure correspond to ions obtained by cleavage of amide bonds. Ions at  $m/z$  775.3 ( $z = 2$ ) and  $m/z$  694.9 ( $z = 2$ ) are because of the loss of one and two  $\text{GlcNH}_2$  residues respectively, indicating *N*-deacetylation occurs on  $\text{GlcNAc}$ . The difference of 89 Da between the ion at  $m/z$  911.4 and the ion at  $m/z$  822.3 corresponds to the loss of one alanine residue from the C-terminal end and establishes the absence of an  $\text{Ala}^4 \rightarrow \text{A}_2\text{pm}^3$  cross-link. The ion at  $m/z$  474.3 in **boldface** corresponds to the  $\text{Glu-A}_2\text{pm-A}_2\text{pm}$  tripeptide and indicates the presence of an  $\text{A}_2\text{pm}^3 \rightarrow \text{A}_2\text{pm}^3$  cross-link.  $\text{GlcNH}_2$ , *N*-deacetylated  $\text{GlcNAc}$ ;  $\text{MurOHNac}$ , *N*-acetylmuramicitol (resulting from the reduction of the  $\text{MurNAc}$  residue).

note, the muropeptide profile of the *C. difficile* 630 $\Delta$ *erm* strain was the same as that of *C. difficile* 630; data not shown).

The RP-HPLC muropeptide profile from *ldt<sub>cd1</sub>* mutant strain (Fig. 1B) exhibited a markedly different profile from that of the 630 $\Delta$ *erm* parental strain. The overall composition of the PG from *ldt<sub>cd1</sub>* shows a significant decrease in muropeptide dimers (56.6 to 29.9%) and an increase in muropeptide monomers (35.1 to 49.8%), whereas the proportion of muropeptide trimers was not significantly affected (Table 2). Among the dimers, a marked decrease (from 41.3 to 19% of all the peaks) of the muropeptides containing a 3  $\rightarrow$  3 cross-link was observed. The proportion of dimers containing a 4  $\rightarrow$  3 cross-link was only slightly decreased (Table 2). A new muropeptide termed Y (10.5% of all the peaks) and two new minor muropeptides termed X (0.9% of all the peaks) and Z (1.8% of all the peaks)

were identified in the HPLC profile of the *ldt<sub>cd1</sub>* mutant strain (Table 1). According to its mass ( $m/z$  1779.5) and MS-MS spectra (Fig. 5), the muropeptide Y could correspond to a dimer with two tetrapeptide stems without a cross-link between the two peptide chains and with a tetrasaccharide chain. Composition analysis fits with the proposed structure as only one  $\text{MurOHNac}$  was detected for two Glu (data not shown). The absence of cleavage of the tetrasaccharide chain by mutanolysin could result from a modification of the central  $\text{MurNAc}$  residue without a change of its mass or from the presence of another type of glycosidic linkage between  $\text{MurNAc}$  and  $\text{GlcNAc}$ . The minor muropeptide X ( $m/z$  1708.5) represents a dimer with a disaccharide tripeptide stem and a disaccharide tetrapeptide stem. The fragmentation pattern of this dimer revealed the same structural features than the muropeptide Y (data not

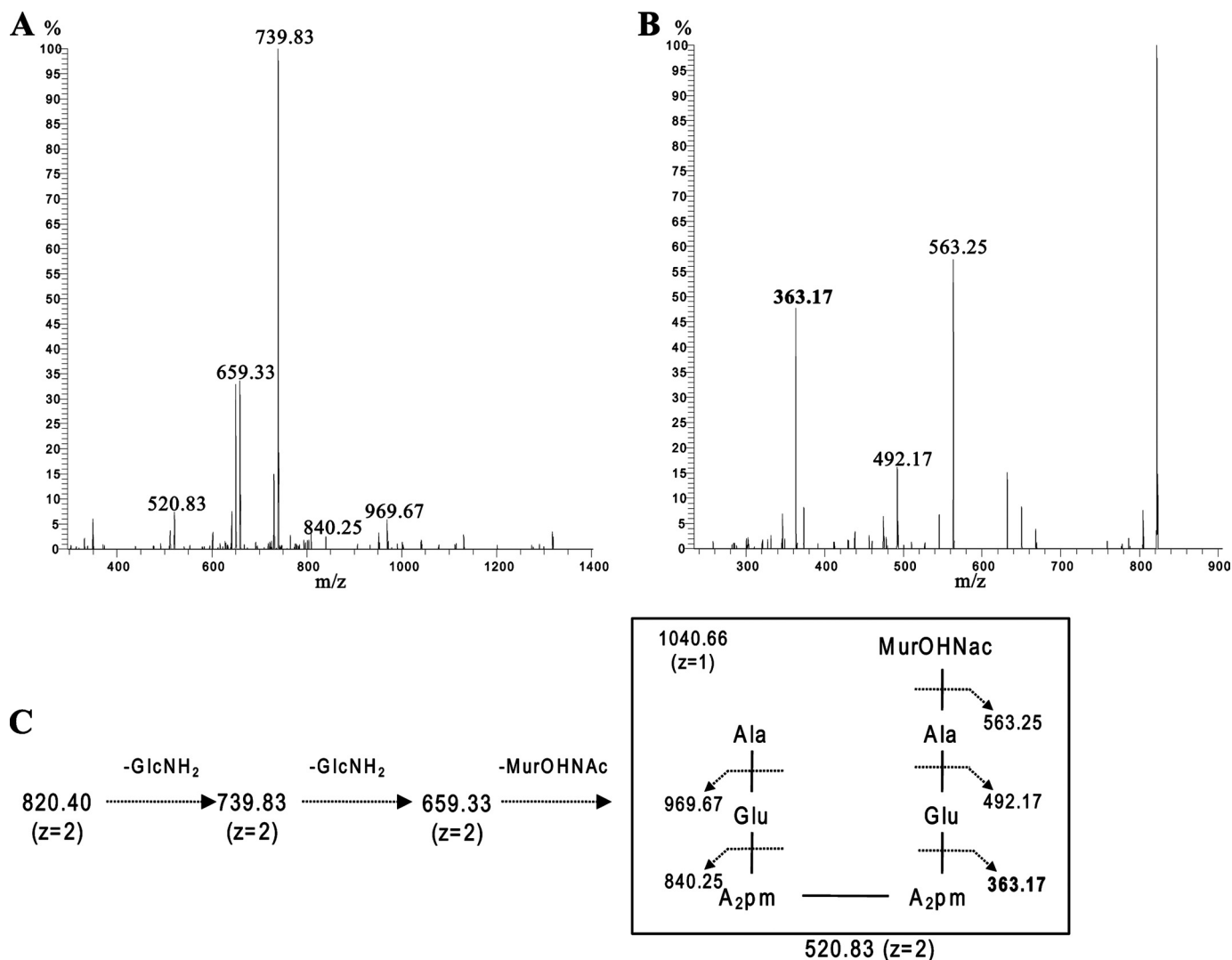


FIGURE 3. **Sequencing of muropeptide 11b by MS-MS.** The muropeptide was desalted and analyzed by MS-MS with a MALDI source. The parental ion ( $m/z$  820.4 with  $z = 2$ ) (A) and the fragment ion  $m/z$  of 840.3 (B) were selected for fragmentation. Inferred structure is represented (C). The indicated  $m/z$  values on the presented structure correspond to ions obtained by cleavage of amide bonds. The ion at  $m/z$  363.2 in **boldface** corresponds to the  $A_2pm-A_2pm$  dipeptide and establishes the presence of an  $A_2pm^3 \rightarrow A_2pm^3$  cross-link. *GlcNH<sub>2</sub>*, *N*-deacetylated *GlcNAc*; *MurOHNAc*, *N*-acetylmuramicitol (resulting from the reduction of the *MurNAc* residue).

shown). By analogy, the structure of the muropeptides Z was assigned to be a trimer with two tetrapeptide stems and a tripeptide stem containing one cross-link generated by transpeptidation and one bond between *MurNAc* and *GlcNAc* residues. Consequently, the overall cross-linking index was only 18.2% in the *ldt<sub>cd1</sub>* mutant strain, compared with 33.8% of the wild type (Table 2). Taken together, these results suggest that *Ldt<sub>cd1</sub>* could function as a *L,D*-transpeptidase involved in the formation of  $A_2pm^3 \rightarrow A_2pm^3$  cross-links.

The muropeptide profile of the *ldt<sub>cd2</sub>* mutant was close to that of the *ldt<sub>cd1</sub>* mutant (data not shown). Indeed, comparison of the PG profile of *ldt<sub>cd2</sub>* mutant with that of the wild type strain revealed an increase of monomers that occurred to the detriment of dimers. The muropeptides involved in this variation of abundance were exactly the same as those listed for the *ldt<sub>cd1</sub>* mutant and led to a significant decrease of cross-links generated by *L,D*-transpeptidation. Moreover, muropeptides X, Y, and Z identified in the *ldt<sub>cd1</sub>* mutant strain were also detected in the PG composition of the *ldt<sub>cd2</sub>* mutant. However, changes

were generally less pronounced in the *ldt<sub>cd2</sub>* mutant strain when compared with the *ldt<sub>cd1</sub>* mutant (Tables 1 and 2).

Cross-link formation of  $A_2pm^3 \rightarrow A_2pm^3$  type was decreased but not abolished either in the *ldt<sub>cd1</sub>* or *ldt<sub>cd2</sub>* mutant strain. This result suggests that there is some functional redundancy, so that *Ldt<sub>cd1</sub>* and *Ldt<sub>cd2</sub>* proteins could have a mutually partial compensatory role. Thus, we determined the muropeptide profile of a *ldt<sub>cd1</sub> ldt<sub>cd2</sub>* double mutant strain. Interestingly, no obvious differences were observed when compared with that of the *ldt<sub>cd1</sub>* mutant strain (Tables 1 and 2). This suggests the involvement of at least a third *L,D*-transpeptidase (possibly CD3007) able to partially compensate for the lack of both *Ldt<sub>cd1</sub>* and *Ldt<sub>cd2</sub>*.

**Impact of Ampicillin on *C. difficile* 630 Peptidoglycan Structure**—The impact of ampicillin on PG structure was evaluated in *C. difficile* 630 grown in the presence of ampicillin at the maximum concentration allowing growth (1.0 mg/liter) (data not shown). Ampicillin did not modify the relative proportion of muropeptide monomers, dimers, and trimers (Table 1). However, ampicillin altered the balance between cross-links



## Peptidoglycan Structure of *Clostridium difficile*

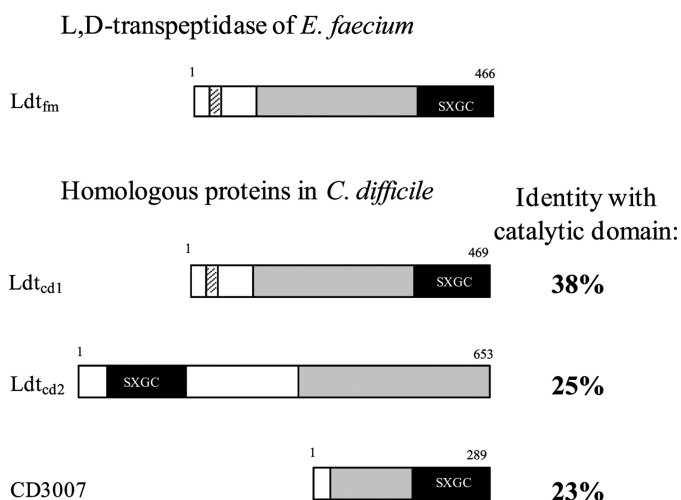


**FIGURE 4. Domain composition of L,D-transpeptidases from *E. faecium* and *C. difficile*.** Hatched boxes represent hydrophobic regions that could act as membrane anchors. Gray and black boxes represent putative peptidoglycan binding domain and the catalytic domain respectively. The sequence of conserved motifs is indicated.

generated by  $D,D$ -transpeptidation and  $L,D$ -transpeptidation. Partial inhibition of the  $D,D$ -transpeptidases by ampicillin decreased the proportion of dimers containing a  $D$ -Ala<sup>4</sup> →  $A_2$ pm<sup>3</sup> cross-link (from 15.3 to 7.4% of all the peaks), leading to an increase of dimers generated by  $L,D$ -transpeptidation (from 41.3 to 48.6% of all the peaks) (Table 2). Thus, 87% of the dimers were cross-linked by  $L,D$ -transpeptidation in the ampicillin-treated strain. This result suggests that  $L,D$ -transpeptidases of *C. difficile* are ampicillin-insensitive. However, *C. difficile* remains susceptible to ampicillin, indicating that  $D,D$ -transpeptidases generating 4–3 cross-links are essential for PG assembly.

**Impact of Vancomycin on *C. difficile* 630 Peptidoglycan Structure**—The genome of *C. difficile* 630 harbors a *vanG*-like operon structure. The *vanG* operon is responsible for moderate resistance to vancomycin in *Enterococcus faecalis* (31), but the *vanG*-like operon does not confer vancomycin resistance in *C. difficile* (25). To investigate if vancomycin could, either directly or through the induction of the *vanG*-like operon, interfere with the  $L,D$ -transpeptidation pathway, we extracted the PG from exponential cultures of *C. difficile* grown in the presence of a subinhibitory concentration of vancomycin (1/4 minimal inhibitory concentration 0.375 mg/liter) and analyzed its structure by RP-HPLC. The muropeptide profile was exactly the same as that of the untreated strain, indicating that vancomycin does not alter the balance between  $L,D$ - and  $D,D$ -transpeptidation mechanisms.

## DISCUSSION

This work reports, for the first time to our knowledge, the composition and structure of PG of *C. difficile*. The most prevalent muropeptide monomer (peak 7, 26.2% of all peaks) (Fig. 1 and Table 1) represents the basic disaccharide tetrapeptide subunit, whose tetrapeptide stem consists of the usual  $L$ -Ala- $D$ -Glu- $A_2$ pm- $D$ -Ala. Of note, some muropeptides (monomer 2 and monomer 10, Table 1) lacked a GlcNAc residue. They could result from cleavage by the previously described Acd glucosaminidase (32). Schleifer and Kandler (33) previously reported the amino acid composition of PG of many species of

the genus *Clostridium*. Most species contained only meso- $A_2$ pm, Ala, and Glu, although *C. perfringens* revealed  $L,L$ - $A_2$ pm instead of meso- $A_2$ pm and additional Gly in the interpeptide bridge, and *Clostridium innocuum* contained  $L$ -Lys instead of  $A_2$ pm. *C. difficile* was not reported in this previous work, but based on our amino acid content detection and on the phylogenetic link of *C. difficile* with *Clostridium bifermentans* and *Clostridium sordellii* (34), which contains meso- $A_2$ pm (33), PG of *C. difficile* very likely contains meso- $A_2$ pm.

A high proportion of  $N$ -deacetylation of the glycan strands was observed in *C. difficile* (Table 1). This structural variation occurred only on GlcNAc residues (Fig. 2), whose 93% were  $N$ -deacetylated, whereas MurNAc residues remained fully acetylated. Nonacetylated glucosamine (GlcN) or muramic acid (MurN) residues have already been reported, but at a lower rate, in some Gram-positive bacteria (29) such as *Bacillus anthracis* (35), *Bacillus subtilis* (36), *S. pneumoniae* (37), or *L. monocytogenes* (21). The presence of these non-acetylated amino sugars confers resistance to lysozyme, an exogenous muramidase, which normally cleaves PG between the glycosidic  $\beta$ 1–4-linked residues of GlcNAc and MurNAc. The  $N$ -deacetylation of the GlcNAc residues is achieved by PgdA deacetylases, which have been shown to provide a protective role against host defenses in *L. monocytogenes* (21) and *S. pneumoniae* (22). Further studies should be performed to examine the impact of GlcNAc  $N$ -deacetylation on lysozyme resistance in *C. difficile*. Our *in silico* analysis of the genome sequence of *C. difficile* 630 revealed the presence of 10 putative polysaccharide deacetylases encoding genes belonging to the carbohydrate esterase family CE4. Ten putative polysaccharide deacetylase-encoding genes were also identified in the *B. anthracis* and *Bacillus cereus* genomes (38), which exhibit important  $N$ -deacetylation levels (29, 35).

An important and unexpected feature of the composition of *C. difficile* PG is the abundance of  $A_2$ pm<sup>3</sup> →  $A_2$ pm<sup>3</sup> cross-links generated by  $L,D$ -transpeptidation. This unusual type of cross-link was originally detected in *E. coli*, in which it represents about 5 and 12% of the total muropeptide content in the exponential and stationary growth phases, respectively (39) and more recently in several Gram-positive bacteria (11, 13, 14, 18). In *Mycobacterium tuberculosis*, the majority of the cross-links are generated by  $D,D$ -transpeptidation during exponential growth, whereas 80% of the cross-links are generated by  $L,D$ -transpeptidation during the stationary growth phase (13). In the present work the PG structure of *C. difficile* from the stationary and exponential growth phases revealed a similar profile, characterized by a large proportion of 3 → 3 cross-links, suggesting that the  $L,D$ -transpeptidases of *C. difficile* constitutively contribute to PG cross-linking. To our knowledge, this predominant contribution of  $L,D$ -transpeptidases to PG cross-linking has never been previously reported in low GC% Gram-positive bacteria.

We identified three putative  $L,D$ -transpeptidases encoding genes, named *ldt<sub>cd1</sub>*, *ldt<sub>cd2</sub>*, and *CD3007* in the genome of *C. difficile* 630 and obtained *ldt<sub>cd1</sub>*, *ldt<sub>cd2</sub>* single and double mutants strains. These genes are significantly transcribed during exponential growth in the wild type strain but are not transcriptionally up-regulated in response to loss of one or more  $L,D$ -transpeptidase-encoding genes in the different mutant strains (data not shown). The PG profiles of the wild type and different  $L,D$ -

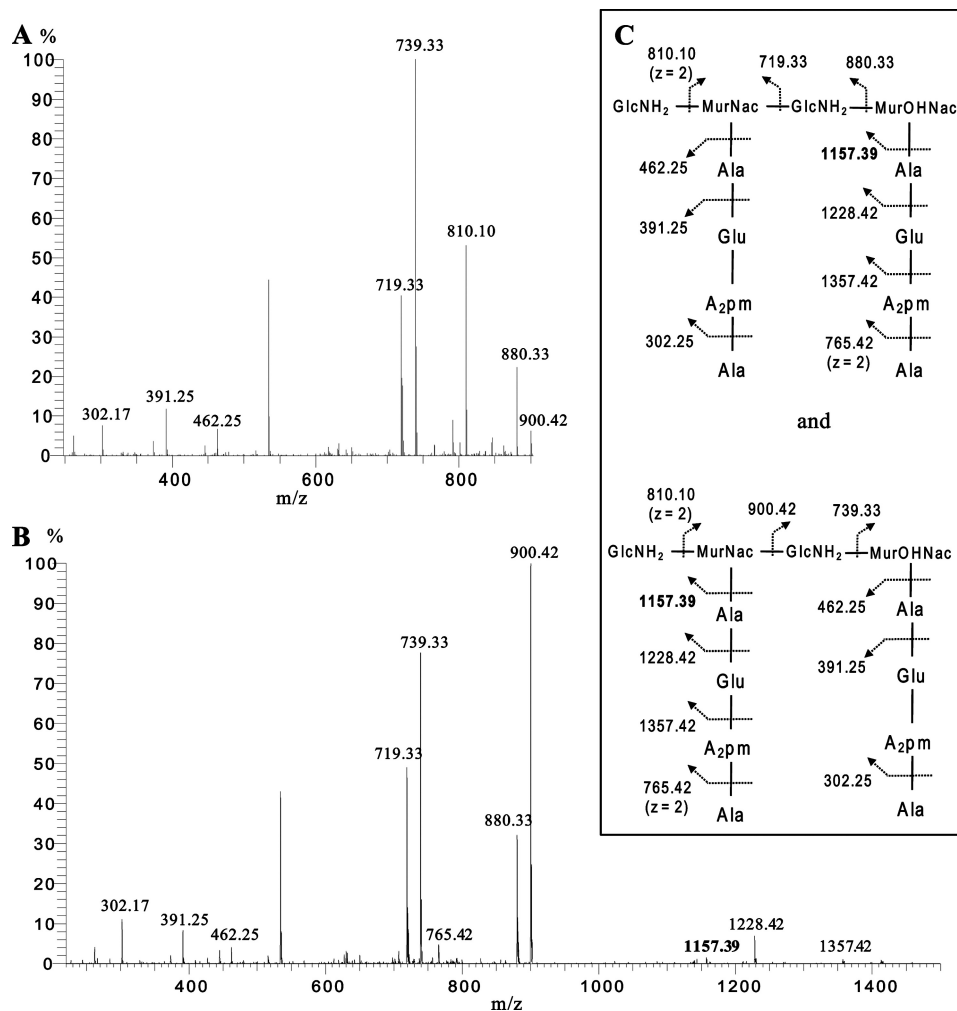


FIGURE 5. **Sequencing of mucopeptide Y by MS-MS.** The mucopeptide was desalted and analyzed by MS-MS with a MALDI source. The parental ion ( $m/z$  890.3 with  $z = 2$ ) (A) and the fragment ion with  $m/z$  of 810.1 ( $z = 2$ ) (B) were selected for fragmentation. Inferred structure is represented (C). The indicated  $m/z$  values on the presented structure correspond to ions obtained by cleavage of amide bonds. The ion at  $m/z$  1157.4 in **boldface** corresponds to a trisaccharide chain (MurNac-GlcNH<sub>2</sub>-MurOHNAc) with a tetrapeptide stem, indicating the absence of cleavage of the MurNac-GlcNH<sub>2</sub> glycosidic bond by mutanolysin. MurOHNAc, *N*-acetylmuramicitol (resulting from the reduction of the MurNac residue); MurNac, the MurNac residue was modified without change of its mass or was involved in an unusual type of glycosidic linkage with GlcNAc, leading to the absence of cleavage of the tetrasaccharide chain by mutanolysin.

transpeptidase mutant strains showed significant differences. The mutant strains show a marked decrease in the abundance of dimers to the partial benefit of monomers. Among the dimers, the proportion of mucopeptides cross-linked by *D,D*-transpeptidation is slightly affected, whereas the proportion of mucopeptides generated by *L,D*-transpeptidation is reduced by about one-half. These modifications lead to a marked decrease of the cross-linking index. Thus, both Ldt<sub>cd1</sub> and Ldt<sub>cd2</sub> constitute functional *L,D*-transpeptidases in *C. difficile*. Of note, mutation of either *ldt<sub>cd1</sub>* or *ldt<sub>cd2</sub>* reduces but does not abolish the formation of A<sub>2</sub>pm<sup>3</sup> → A<sub>2</sub>pm<sup>3</sup> cross-links, and the mucopeptide profile of a double mutant strain lacking both Ldt<sub>cd1</sub> and Ldt<sub>cd2</sub> is similar to that of the single mutant strains. These data indicate the presence of at least a third functional *L,D*-transpeptidase (possibly CD3007) that could partially compensate for the loss of Ldt<sub>cd1</sub> and Ldt<sub>cd2</sub> encoding genes.

Another notable feature of the PG structure of Ldt<sub>cd1</sub> and Ldt<sub>cd2</sub> mutants is the presence of three new mucopeptides. Two of them have a dimeric structure with one tetrapeptide and one tripeptide side chain or two tetrapeptide side chains, whereas

the third has a trimeric structure with one tripeptide and two tetrapeptide side chains. Interestingly, MS-MS sequencing of the new mucopeptide dimers revealed the absence of a peptide cross-link but the presence of a bond between the MurNac residue of the first disaccharide and the GlcNAc residue of the second disaccharide. It appears that the glycosidic bond between the MurNac and GlcNH<sub>2</sub> residues of the new mucopeptides are insensitive to the mutanolysin activity. It was reported in *B. subtilis* that the glycosidic bond adjacent to a muramic  $\delta$ -lactam in endospore PG is resistant to the action of muramidases (40, 41). However, in *C. difficile*, the mechanism of the mutanolysin resistance remains unclear and could result from a change in the MurNac residue or from the formation of an unusual glycosidic bond.

The relative contribution of *D,D*-transpeptidation and *L,D*-transpeptidation for cross-linking has been related to ampicillin resistance in *E. faecium* (42). Partial inhibition of the *D,D*-transpeptidases by ampicillin increased the proportion of the dimeric mucopeptides containing an A<sub>2</sub>pm<sup>3</sup> → A<sub>2</sub>pm<sup>3</sup> cross-link, suggesting that the *L,D*-transpeptidation pathway is insen-

## Peptidoglycan Structure of *Clostridium difficile*

sitive to ampicillin in *C. difficile*. However, despite a predominant amount of 3-3 cross-links, *C. difficile* remains susceptible to ampicillin (although minimal inhibitory concentration values are higher than in species such as *C. perfringens*) (24). These observations suggest that the residual D<sub>3</sub>D-transpeptidase activity of penicillin-binding proteins detected in the presence of ampicillin could be essential to the PG assembly of *C. difficile*.

The activity of the Ldt<sub>fm</sub> L<sub>3</sub>D-transpeptidase in *E. faecium* is limited by the production of its tetrapeptide substrate (10), which results from the activity of a  $\beta$ -lactam insensitive metallo-D<sub>3</sub>D-carboxypeptidase named DdcY and belonging to the VanY superfamily (43). In *C. difficile*, the impact of ampicillin on the PG structure suggests the presence of a homologous gene to the DdcY encoding gene responsible for the tetrapeptide substrate production. The genome of *C. difficile* harbors three putative  $\beta$ -lactams-insensitive D<sub>3</sub>D-carboxypeptidases, generating tetrapeptide substrate. Among them, VanXY<sub>G</sub> is encoded by a member of the *vanG*-like operon that does not confer resistance to vancomycin. Further studies should be considered to investigate the involvement of the different D<sub>3</sub>D-carboxypeptidases in the tetrapeptide substrate production, which is critical for the main 3-3 cross-linking in *C. difficile*. This study shows that *C. difficile* displays an original PG structure including a high level of *N*-deacetylated GlcNAc and a predominant proportion of 3 → 3 cross-links generated by at least two L<sub>3</sub>D-transpeptidases.

*Acknowledgments*—We thank Nigel P. Minton and John T. Heap as creators of the *ClosTron* gene knockout system and Bruno Dupuy for the gift of the strain 630 $\Delta$ erm of *C. difficile*.

### REFERENCES

1. Viswanathan, V. K., Mallozzi, M. J., and Vedantam, G. (2010) *Gut Microbes* **1**, 234–242
2. Finegold, S. M. (1986) *Scand. J. Infect Dis. Suppl.* **49**, 160–164
3. Kelly, C. P., and LaMont, J. T. (1998) *Annu. Rev. Med.* **49**, 375–390
4. Voth, D. E., and Ballard, J. D. (2005) *Clin. Microbiol. Rev.* **18**, 247–263
5. Höltje, J. V. (1998) *Microbiol. Mol. Biol. Rev.* **62**, 181–203
6. Scheffers, D. J., and Pinho, M. G. (2005) *Microbiol. Mol. Biol. Rev.* **69**, 585–607
7. Sauvage, E., Kerff, F., Terrak, M., Ayala, J. A., and Charlier, P. (2008) *FEMS Microbiol. Rev.* **32**, 234–258
8. Zapun, A., Contreras-Martel, C., and Vernet, T. (2008) *FEMS Microbiol. Rev.* **32**, 361–385
9. Mainardi, J. L., Villet, R., Bugg, T. D., Mayer, C., and Arthur, M. (2008) *FEMS Microbiol. Rev.* **32**, 386–408
10. Mainardi, J. L., Fourgeaud, M., Hugonnet, J. E., Dubost, L., Brouard, J. P., Ouazzani, J., Rice, L. B., Gutmann, L., and Arthur, M. (2005) *J. Biol. Chem.* **280**, 38146–38152
11. Lavollay, M., Arthur, M., Fourgeaud, M., Dubost, L., Marie, A., Riegel, P., Gutmann, L., and Mainardi, J. L. (2009) *Mol. Microbiol.* **74**, 650–661
12. Magnet, S., Arbeloa, A., Mainardi, J. L., Hugonnet, J. E., Fourgeaud, M., Dubost, L., Marie, A., Delfosse, V., Mayer, C., Rice, L. B., and Arthur, M. (2007) *J. Biol. Chem.* **282**, 13151–13159
13. Lavollay, M., Arthur, M., Fourgeaud, M., Dubost, L., Marie, A., Veziris, N., Blano, D., Gutmann, L., and Mainardi, J. L. (2008) *J. Bacteriol.* **190**, 4360–4366
14. Lavollay, M., Fourgeaud, M., Herrmann, J. L., Dubost, L., Marie, A., Gutmann, L., Arthur, M., and Mainardi, J. L. (2011) *J. Bacteriol.* **193**, 778–782
15. Gupta, R., Lavollay, M., Mainardi, J. L., Arthur, M., Bishai, W. R., and Lamichhane, G. (2010) *Nat. Med.* **16**, 466–469
16. Magnet, S., Bellais, S., Dubost, L., Fourgeaud, M., Mainardi, J. L., Petit-Frère, S., Marie, A., Mengin-Lecreulx, D., Arthur, M., and Gutmann, L. (2007) *J. Bacteriol.* **189**, 3927–3931
17. Magnet, S., Dubost, L., Marie, A., Arthur, M., and Gutmann, L. (2008) *J. Bacteriol.* **190**, 4782–4785
18. Mainardi, J. L., Legrand, R., Arthur, M., Schoot, B., van Heijenoort, J., and Gutmann, L. (2000) *J. Biol. Chem.* **275**, 16490–16496
19. Vollmer, W. (2008) *FEMS Microbiol. Rev.* **32**, 287–306
20. Bernard, E., Rolain, T., Courtin, P., Guillot, A., Langella, P., Hols, P., and Chapot-Chartier, M. P. (2011) *J. Biol. Chem.* **286**, 23950–23958
21. Boneca, I. G., Dussurget, O., Cabanes, D., Nahori, M. A., Sousa, S., Lecuit, M., Psylinakis, E., Bouriotis, V., Hugot, J. P., Giovannini, M., Coyle, A., Bertin, J., Namane, A., Rousselle, J. C., Cayet, N., Prévost, M. C., Balloy, V., Chignard, M., Philpott, D. J., Cossart, P., and Girardin, S. E. (2007) *Proc. Natl. Acad. Sci. U.S.A.* **104**, 997–1002
22. Vollmer, W., and Tomasz, A. (2002) *Infect Immun.* **70**, 7176–7178
23. Bera, A., Herbert, S., Jakob, A., Vollmer, W., and Götz, F. (2005) *Mol. Microbiol.* **55**, 778–787
24. Citron, D. M., Merriam, C. V., Tyrrell, K. L., Warren, Y. A., Fernandez, H., and Goldstein, E. J. (2003) *Antimicrob. Agents Chemother.* **47**, 2334–2338
25. Sebahia, M., Wren, B. W., Mullany, P., Fairweather, N. F., Minton, N., Stabler, R., Thomson, N. R., Roberts, A. P., Cerdeño-Tárraga, A. M., Wang, H., Holden, M. T., Wright, A., Churcher, C., Quail, M. A., Baker, S., Bason, N., Brooks, K., Chillingworth, T., Cronin, A., Davis, P., Dowd, L., Fraser, A., Feltwell, T., Hance, Z., Holroyd, S., Jagels, K., Moule, S., Mungall, K., Price, C., Rabinowitsch, E., Sharp, S., Simmonds, M., Stevens, K., Unwin, L., Whithead, S., Dupuy, B., Dougan, G., Barrell, B., and Parkhill, J. (2006) *Nat. Genet.* **38**, 779–786
26. Hussain, H. A., Roberts, A. P., and Mullany, P. (2005) *J. Med. Microbiol.* **54**, 137–141
27. Courtin, P., Miranda, G., Guillot, A., Wessner, F., Mézange, C., Domakova, E., Kulakauskas, S., and Chapot-Chartier, M. P. (2006) *J. Bacteriol.* **188**, 5293–5298
28. Heap, J. T., Pennington, O. J., Cartman, S. T., Carter, G. P., and Minton, N. P. (2007) *J. Microbiol. Methods* **70**, 452–464
29. Vollmer, W., Blanot, D., and de Pedro, M. A. (2008) *FEMS Microbiol. Rev.* **32**, 149–167
30. Bielnicki, J., Devedjiev, Y., Derewenda, U., Dauter, Z., Joachimiak, A., and Derewenda, Z. S. (2006) *Proteins* **62**, 144–151
31. Depardieu, F., Bonora, M. G., Reynolds, P. E., and Courvalin, P. (2003) *Mol. Microbiol.* **50**, 931–948
32. Dhalluin, A., Bourgeois, I., Pestel-Caron, M., Camiade, E., Raux, G., Courtin, P., Chapot-Chartier, M. P., and Pons, J. L. (2005) *Microbiology* **151**, 2343–2351
33. Schleifer, K. H., and Kandler, O. (1972) *Bacteriol. Rev.* **36**, 407–477
34. Collins, M. D., Lawson, P. A., Willems, A., Cordoba, J. J., Fernandez-Garayzabal, J., Garcia, P., Cai, J., Hippe, H., and Farrow, J. A. (1994) *Int. J. Syst. Bacteriol.* **44**, 812–826
35. Zipperle, G. F., Jr., Ezzell, J. W., Jr., and Doyle, R. J. (1984) *Can. J. Microbiol.* **30**, 553–559
36. Atrih, A., Bacher, G., Allmaier, G., Williamson, M. P., and Foster, S. J. (1999) *J. Bacteriol.* **181**, 3956–3966
37. Vollmer, W., and Tomasz, A. (2000) *J. Biol. Chem.* **275**, 20496–20501
38. Psylinakis, E., Boneca, I. G., Mavromatis, K., Deli, A., Hayhurst, E., Foster, S. J., Vårum, K. M., and Bouriotis, V. (2005) *J. Biol. Chem.* **280**, 30856–30863
39. Pisabarro, A. G., de Pedro, M. A., and Vázquez, D. (1985) *J. Bacteriol.* **161**, 238–242
40. Warth, A. D., and Strominger, J. L. (1972) *Biochemistry* **11**, 1389–1396
41. Atrih, A., Zöllner, P., Allmaier, G., and Foster, S. J. (1996) *J. Bacteriol.* **178**, 6173–6183
42. Mainardi, J. L., Morel, V., Fourgeaud, M., Cremniter, J., Blanot, D., Legrand, R., Frehel, C., Arthur, M., Van Heijenoort, J., and Gutmann, L. (2002) *J. Biol. Chem.* **277**, 35801–35807
43. Sacco, E., Hugonnet, J. E., Josseaume, N., Cremniter, J., Dubost, L., Marie, A., Patin, D., Blanot, D., Rice, L. B., Mainardi, J. L., and Arthur, M. (2010) *Mol. Microbiol.* **75**, 874–885
44. Glauner, B., Höltje, J. V., and Schwarz, U. (1988) *J. Biol. Chem.* **263**, 10088–10095

***Clostridium difficile* Has an Original Peptidoglycan Structure with a High Level of N-Acetylglucosamine Deacetylation and Mainly 3-3 Cross-links**

Johann Peltier, Pascal Courtin, Imane El Meouche, Ludovic Lemée, Marie-Pierre Chapot-Chartier and Jean-Louis Pons

*J. Biol. Chem.* 2011, 286:29053-29062.

doi: 10.1074/jbc.M111.259150 originally published online June 17, 2011

---

Access the most updated version of this article at doi: [10.1074/jbc.M111.259150](https://doi.org/10.1074/jbc.M111.259150)

Alerts:

- [When this article is cited](#)
- [When a correction for this article is posted](#)

[Click here](#) to choose from all of JBC's e-mail alerts

Supplemental material:

<http://www.jbc.org/content/suppl/2011/06/17/M111.259150.DC1>

This article cites 44 references, 23 of which can be accessed free at <http://www.jbc.org/content/286/33/29053.full.html#ref-list-1>